A control-oriented wave-excited linear model for offshore floating wind turbines

Fontanella, A.; Al, M.; Van Der Hoek, D.; Liu, Y.; Van Wingerden, J. W.; Belloli, M.

DOI
10.1088/1742-6596/1618/2/022038

Publication date
2020

Document Version
Final published version

Published in
Journal of Physics: Conference Series

Journal of Physics: Conference Series

PAPER • OPEN ACCESS

A control-oriented wave-excited linear model for offshore floating wind turbines

To cite this article: A. Fontanella *et al* 2020 *J. Phys.: Conf. Ser.* **1618** 022038

Journal of Physics: Conference Series **1618** (2020) 022038 doi:10.1088/1742-6596/1618/2/022038

A control-oriented wave-excited linear model for offshore floating wind turbines

A. Fontanella[1], M. Al[2], D. van der Hoek[2], Y. Liu[2], J.W. van Wingerden[2], M. Belloli[1]

[1] Mechanical Engineering Department, Politecnico di Milano, Milano, Via La Masa 1, 20156, Italy.

[2] Delft Center for Systems and Control, Delft University of Technology, Delft, 2628 CD, The Netherlands.

E-mail: alessandro.fontanella@polimi.it

Abstract. The design of control strategies for floating offshore wind turbines (FOWTs) is even more difficult than for onshore and bottom-fixed offshore ones and a recognized control strategy for FOWTs is currently lacking. In order to design effective control strategies, the additional dynamics of these systems should be taken into account in the models used to solve this task. This paper presents the analytical derivation of a novel model conceived for control design purposes. In detail, the model is based on a linear description of the highly non-linear phenomena that are relevant for an FOWT. The quasi-steady assumption is used to give a description of the aerodynamic loads and how these are influenced by the main control inputs. Hydrodynamic radiation and diffraction forces are introduced by means of linear-time-invariant parametric models. Simulation results shows that the proposed linear model is able to predict the structural response of the turbine system and the floating platform effectively in the case of control inputs, wind and wave disturbances. Compared to the nonlinear high-fidelity model, the proposed model shows similar results, however, without much complexity, which is promising in the desing of FOWT control strategies.

1. Introduction

Nowadays, floating wind is a recognized technology representing the key to harvest the abundant deep-water wind energy resource. When deploying a multi-megawatt wind turbine on a floating foundation instead of a bottom-fixed one, additional engineering challenges emerge, which should be addressed. Controlling the wind turbine is among these, since it has been widely proven that control logics developed for onshore and bottom-fixed systems are not effective for floating offshore wind turbines (FOWTs). In order to reach this goal, control-oriented models are required. These models simplify the physics of an FOWT to a certain extent in order to get a description of the sole dynamics that are deemed to be important for the synthesis of a control logic. Such control-oriented FOWT models are currently lacking. Simulation codes mainly operate in the time domain and provide a high-fidelity representation of the floating system and the involved non-linear dynamics. A large amount of parameters is usually required to feed the model and the obtained FOWT representation is not suitable to be used with the most common control design techniques.

Reduced-order models are widely used whenever fidelity can be reduced [1, 2, 3]. These are often obtained from a linearization and order reduction of high-fidelity non-linear models. A survey of state-of-the-art techniques used to solve this task is reported in [4]. To approach the shortage of control-oriented models, a novel wave-excited linear model is developed in this paper. In detail, the proposed model is derived by the analytical approach with a linear formulation. Based on this, the multi-physics dynamics of the FOWT for any given operation condition can be successfully approximated. Few parameters are required to feed the model and the obtained representation of the floating system can be readily included in control design algorithms. The model is also very efficient from a computational point of view making it an appropriate base of floating wind farm models.

This paper is organized as follows. In Section 2 the wave-excited linear model is presented, introducing the analytical equations that are adopted to describe the FOWT physics. In Section 3 the novel linear model is tested against a FAST v8.16 counterpart assuming a 10MW FOWT as a case study. In Section 4 the capabilities of the novel model are illustrated studying the implementation of a pitch-to-feather control strategy. The paper ends with conclusions in Section 5.

2. The wave-excited linear model

The wave-excited linear model is developed to characterize the dynamics of the FOWT around a generic steady-state configuration set by an average wind speed, static displacement of the platform, rotor speed, collective pitch, generator torque.

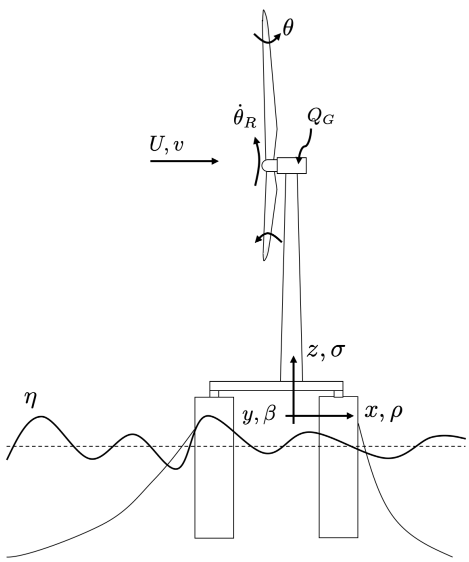

Figure 1. Scheme of the modeled FOWT.

2.1. *Structural model*

It is assumed that the FOWT is formed by rigid bodies which relative position is restricted by geometric constraints. The rotor is upwind and the tilt angle is neglected. Under these hypotheses the equations of motions (EOMs) for the system are derived by means of the Lagrange's theorem.

Regarding the rotor dynamics, the EOM of the rotor is:

$$(J_R + \tau^2 J_G)\ddot{\theta}_R = Q_{aero} - \tau Q_G \,, \tag{1}$$

where θ_R is the azimuth, J_R is the rotor (hub and blades) inertia, τ is the transmission ratio (high-speed to low-speed), J_G the generator inertia, Q_{aero} the rotor aerodynamic torque and Q_G the generator torque.

In addition, the EOMs for the independent coordinates corresponding to the FOWT rigid-body degrees of freedom (DOFs) $\boldsymbol{\xi} = (x, y, z, \rho, \beta, \sigma)^T$, namely surge, sway, heave, roll, pitch, yaw, can be derived by means of the multi-body dynamics theory [5] as:

$$\boldsymbol{M}_{RB}\ddot{\boldsymbol{\xi}} + \boldsymbol{K}_{RB}\boldsymbol{\xi} = \boldsymbol{F}\,, \tag{2}$$

where $\boldsymbol{M}_{RB}$ and $\boldsymbol{K}_{RB}$ are the FOWT inertia and gravitational stiffness matrix, $\boldsymbol{F}$ the generalized force vector for the six DOFs including five components:

$$\boldsymbol{F} = \boldsymbol{F}_b + \boldsymbol{F}_{moor} + \boldsymbol{F}_{rad} + \boldsymbol{F}_{wave} + \boldsymbol{F}_{aero}\,, \tag{3}$$

that are restoring due to buoyancy, due to the mooring system, hydrodynamic radiation, wave excitation and aerodynamic forces.

2.2. Restoring loads

Restoring forces that arise on the FOWT due to buoyancy are introduced in the model as:

$$\boldsymbol{F}_b = -\boldsymbol{G}_B\boldsymbol{\xi}\,, \tag{4}$$

where $\boldsymbol{G}_B$ is the linear hydrostatic-restoring matrix that relates a change in the displaced volume of water to a change in the buoyancy restoring forces and $\boldsymbol{\xi}$ is the variation of FOWT position with respect to a generic static equilibrium position.

Additional restoring loads are exerted on the floating platform by the mooring system. A variety of models featured by different degrees of complexity exists to simulate the mooring system and predict the forces exerted on the FOWT [6, 7, 8]. However, these models are too complex when deriving a control-oriented linear model of the FOWT. The position-dependent component of the mooring force is large with respect to the mooring inertia and hydrodynamic loads, which are meaningful only when the analysis is focused on the mooring line itself and can be neglected when studying the global dynamics of the FOWT [9]. Moreover, the force-position relation for a catenary mooring is in good approximation linear for a wide range of operation conditions. Under these assumptions, the total load exerted by the mooring system on the floating platform is:

$$\boldsymbol{F}_{moor} = -\boldsymbol{G}_{moor}\boldsymbol{\xi}\,, \tag{5}$$

where $\boldsymbol{G}_{moor}$ is the linear restoring matrix from all the mooring lines and $\boldsymbol{\xi}$ is as before.

2.3. Radiation loads

According to Cummins [10] the hydrodynamic radiation loads are expressed by the following time domain relation:

$$\boldsymbol{F}_{rad} = -\boldsymbol{A}_\infty\ddot{\boldsymbol{\xi}} - \int_0^t \boldsymbol{K}(t-t')\dot{\boldsymbol{\xi}}(t')dt' = -\boldsymbol{A}_\infty\ddot{\boldsymbol{\xi}} - \boldsymbol{\mu}(t)\,. \tag{6}$$

The forces due to the body acceleration are represented by the first term and the constant positive-definite infinite frequency added mass matrix $\boldsymbol{A}_\infty$. The frequency-dependent added mass and damping associated with the fluid memory effect are given by the convolution integral and the kernel $\boldsymbol{K}(t)$ is the matrix of retardation functions (impulse responses). Considering radiation forces in the frequency domain it is possible to relate the impulse responses and the frequency dependent added mass and damping [11]:

$$\boldsymbol{K}(\omega) = \boldsymbol{B}(\omega) + j\omega(\boldsymbol{A}(\omega) - \boldsymbol{A}_{\infty})\,. \tag{7}$$

The frequency dependent added damping $\boldsymbol{B}(\omega)$, mass $\boldsymbol{A}(\omega)$ and the infinite frequency added mass $\boldsymbol{A}_{\infty}$ matrices are commonly computed by means of hydrodynamic codes based on potential theory [12].

The non-parametric radiation model of equation 6 and its convolution integral are not suitable for developing a linear model of an FOWT. It is worth noticing that the convolution integral is a linear operator and can be approximated by a parametric linear time-invariant (LTI) model in state-space form as in equation 8. This can be established by means of the system identification technique based on the frequency response data (FRD) in the form of equation 7.

$$\begin{cases} \dot{\boldsymbol{x}}_r = \hat{\boldsymbol{A}}_r \boldsymbol{x}_r + \hat{\boldsymbol{B}}_r \dot{\boldsymbol{\xi}} \\ \hat{\boldsymbol{\mu}} = \hat{\boldsymbol{C}}_r \boldsymbol{x}_r \end{cases} , \tag{8}$$

where the number of states in $\boldsymbol{x}_r$ is the order of the approximating system, $\hat{\boldsymbol{\mu}}$ is an estimate of $\boldsymbol{\mu}$ and $\hat{\boldsymbol{A}}_r$, $\hat{\boldsymbol{B}}_r$, $\hat{\boldsymbol{C}}_r$ are critical matrices derived from the frequency domain system identification of the non-parametric FRD. In this work, the frequency domain identification method of the *MATLAB* toolbox developed in [13] is used for the identification of the parametric radiation model.

2.4. Wave loads

The forces due to incident waves $\boldsymbol{F}_{wave}$ are the sum of the Froude-Krylov force and the wave diffraction. It can be written in the frequency domain form by:

$$\boldsymbol{F}_{wave}(\omega) = \boldsymbol{X}(\omega)\eta(\omega)\,, \tag{9}$$

where the first term on the right-hand side is the wave force coefficients vector determined by the platform geometry and the wave heading direction and the second denotes the complex spectrum of the wave elevation at the platform location.

In the majority of FOWT simulation codes wave excitation forces are introduced as time series computed prior to simulation from the inverse Fourier transform of equation 9 for an assigned wave spectrum. This representation is not an effective way to build the control-oriented linear model in the frequency-domain.

As suggested in [14], a more suitable representation can be obtained by approximating the non-parametric wave force coefficients vector via the LTI parametric model in a state-space form. This, namely the the wave excitation model (WEM) in this paper, is described in equation 10.

$$\begin{cases} \dot{\boldsymbol{x}}_w = \hat{\boldsymbol{A}}_w \boldsymbol{x}_w + \hat{\boldsymbol{B}}_w \eta \\ \boldsymbol{F}_{wave} = \hat{\boldsymbol{C}}_w \boldsymbol{x}_w \end{cases} , \tag{10}$$

where the number of states in $\boldsymbol{x}_w$ defines the order of the approximating parametric model, whereas $\hat{\boldsymbol{A}}_w$, $\hat{\boldsymbol{B}}_w$, $\hat{\boldsymbol{C}}_w$ are critical matrices by implementing the system identification on the non-parametric data $\boldsymbol{X}(\omega)$.

To behave according to the law of physics some properties have to be enforced in the identified model as constraints for the identification procedure or for the WEM structure. In [14] a WEM is identified with the properties of causality, stability, passivity and relative degree $r \geq 1$. No requirements are set for the low-frequency behavior. However, the presence of a nonzero steady-state amplification in the identified WEM may result into an excessively large excitation of the FOWT rigid-body modes and it is therefore preferable to have a zero gain for low frequencies. The wave force coefficients $\boldsymbol{X}(\omega)$ describe a not causal system [15]. This is because these are defined in panel codes as the ratio between the FRF of the wave forces and the wave elevation at platform location, but forces are generated as soon as the wave impacts the platform and before it reaches the platform location. Since it makes easier to cast the causality property in the parametric model, time-domain identification was preferred over frequency-domain identification. Based on these consideration, the following system identification procedure is proposed to obtain the WEM:

(i) the time domain realization of the wave force coefficients is obtained computing the inverse Fourier transform of the original FRD (i.e. the impulse response);
(ii) the impulse response is delayed t_d seconds, where t_d is the arbitrary time shift to have a small enough response for negative times;
(iii) zero gain for low frequencies is obtained by forcing the model to have a zero at zero frequency; this property is achieved integrating the shifted impulse response in time-domain before identification and augmenting the identified model with a differentiator;
(iv) the *n4sid* subspace identification method is used to identify an initial model that is then refined using the prediction-error minimization (PEM) technique.

2.5. Aerodynamic loads

From the control-oriented model point of view, the rotor can be modeled as a point coincident with the hub location that produces a torque Q_{aero} and a thrust force T_{aero} [8, 16, 17]. The aerodynamic loads are computed from a set of aerodynamic coefficients for any combination of rotor speed, wind speed and collective pitch angle. According to a quasi-steady approach, the variation of the aerodynamic torque and thrust from their steady-state values is obtained from the widely-used first order Taylor expansion of their generic expression:

$$\begin{cases} Q_{aero} = K_{\omega Q}\omega_R + K_{\theta Q}\theta + K_{vQ}V \\ T_{aero} = K_{\omega T}\omega_R + K_{\theta T}\theta + K_{vT}V \end{cases}, \tag{11}$$

where $K_{\omega Q}$, $K_{\theta Q}$, K_{vQ} and $K_{\omega T}$, $K_{\theta T}$, K_{vT} are the partial derivatives of the torque and thrust coefficients with respect rotor speed, collective pitch and wind speed (subscripts ω, θ and v respectively). These are often referred to as rotor sensitivities [18]. Rotor sensitivities change according to the wind turbine operation condition identified by a value of rotor speed, collective pitch and wind speed. The first two variables are uniquely related to the mean wind speed by the control scheme adopted for power regulation. The generic sensitivity $K_{ij}(U)$ describes how the j force varies due to a variation of the i parameter in the neighborhood of the operation condition identified by the mean wind speed U.

The effective wind speed variation V at the hub-height h is caused by the horizontal turbulence v and the hub velocity U_{hub} in the streamwise direction. In particular, the assumption is made here that U_{hub} is only induced by the surge and pitch motions of the floating platform.

$$V = v - (\dot{x} + \dot{\beta}h)\,. \tag{12}$$

The rotor torque is therefore introduced in the linear model as:

$$Q_{aero}(U) = K_{\omega Q}(U)\omega_R + K_{\theta Q}(U)\theta + K_{vQ}(U)v - K_{vQ}(U)\dot{x} - hK_{vQ}(U)\dot{\beta}\,. \tag{13}$$

The generalized force vector due to rotor thrust for the six platform DOFs is:

$$\boldsymbol{F}_{aero}(U) = \boldsymbol{C}_A(U)\dot{\boldsymbol{\xi}} + \boldsymbol{H}_A(U)\boldsymbol{u}_A\,, \tag{14}$$

where the $\boldsymbol{C}_A$ and $\boldsymbol{H}_A$ matrices are function of the rotor sensitivities at the considered operation condition and so of the mean wind speed. Vector $\boldsymbol{u}_A = [\theta, v]^T$ is an input for the model.

Journal of Physics: Conference Series **1618** (2020) 022038 doi:10.1088/1742-6596/1618/2/022038

2.6. The state-space model

All the structural, hydrodynamic and aerodynamic models can be incorporated into a generalized state-space representation as:

$$\underbrace{\begin{bmatrix} \ddot{\theta}_R \\ \ddot{\boldsymbol{\xi}} \\ \dot{\boldsymbol{\xi}} \\ \hline \dot{\boldsymbol{x}}_r \\ \dot{\boldsymbol{x}}_w \end{bmatrix}}_{\dot{\boldsymbol{x}}} = \underbrace{\left[\begin{array}{c|cc} \boldsymbol{A}_1(U) & \begin{matrix}\boldsymbol{0} \\ \boldsymbol{B}_2\boldsymbol{C}_r\end{matrix} & \begin{matrix}\boldsymbol{0} \\ \boldsymbol{B}_3\boldsymbol{C}_w\end{matrix} \\ \hline \begin{matrix}\boldsymbol{0} & \boldsymbol{B}_r \\ \boldsymbol{0} & \boldsymbol{0}\end{matrix} & \begin{matrix}\boldsymbol{A}_r \\ \boldsymbol{0}\end{matrix} & \begin{matrix}\boldsymbol{0} \\ \boldsymbol{A}_w\end{matrix} \end{array}\right]}_{\boldsymbol{A}} \underbrace{\begin{bmatrix} \dot{\theta}_R \\ \dot{\boldsymbol{\xi}} \\ \boldsymbol{\xi} \\ \hline \boldsymbol{x}_r \\ \boldsymbol{x}_w \end{bmatrix}}_{\boldsymbol{x}} + \underbrace{\begin{bmatrix} \boldsymbol{B}_1(U) \\ \hline \boldsymbol{0} \\ \boldsymbol{0} \end{bmatrix}}_{\boldsymbol{B}} \underbrace{\begin{bmatrix} \theta \\ v \\ Q_G \\ \eta \end{bmatrix}}_{\boldsymbol{u}} . \tag{15}$$

The state vector $\boldsymbol{x}$ comprises physical states for the FOWT DOFs $(\dot{\theta}_R, \dot{\boldsymbol{\xi}}, \boldsymbol{\xi})^T$and additional states required for representing hydrodynamic radiation $\boldsymbol{x}_r$ and wave excitation $\boldsymbol{x}_w$. $\boldsymbol{A}_1(U)$ and $\boldsymbol{B}_1(U)$ collect the terms associated with the wind turbine aerodynamics and give the model dependency from the wind turbine operation condition, thus from the average wind speed. The inputs are the deviations of collective pitch angle and generator torque from their steady-state value, horizontal turbulence and the wave elevation. The linear model of equation 15 can be used for time-domain simulation as well as to compute the FOWT transfer functions.

3. Model verification

The model capabilities with respect to the prediction of an FOWT response to wind, waves and control inputs are verified via a case study. The floating system formed by the DTU 10MW wind turbine [19] and the TripleSpar floating platform [20] is implemented with the linear model and with FAST v8.16. The latter is a higher-order nonlinear model and represents the benchmark.

The proposed formulation for introducing wave excitation loads is exemplified in figure 2 where a WEM for zero-degree heading waves is identified for the TripleSpar floating platform [20]. Moreover, the rotor sensitivities of the DTU 10MW reference wind turbine [19] are illustrated in figure 3.

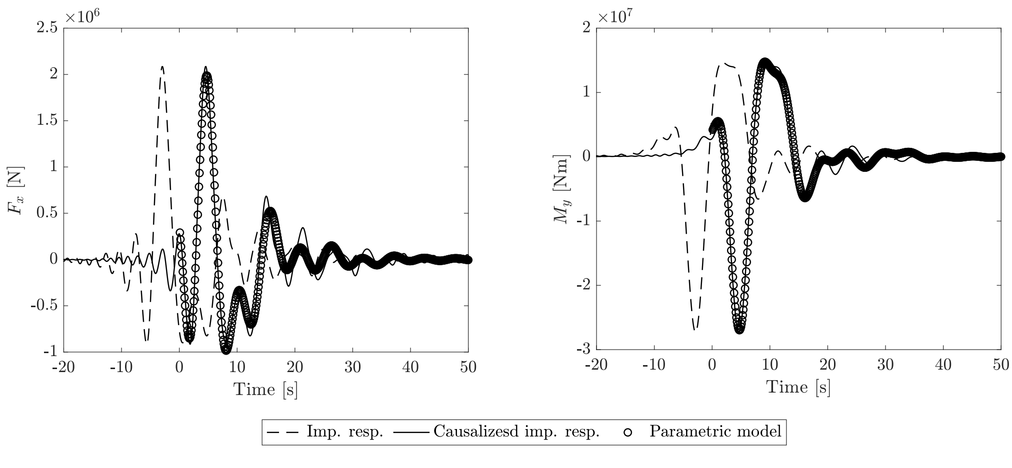

Figure 2. Wave surge force and pitch moment impulse response, causalized impulse response ($t_d = 7.5$ s) and parametric model fit (6 states) of the TripleSpar floating platform.

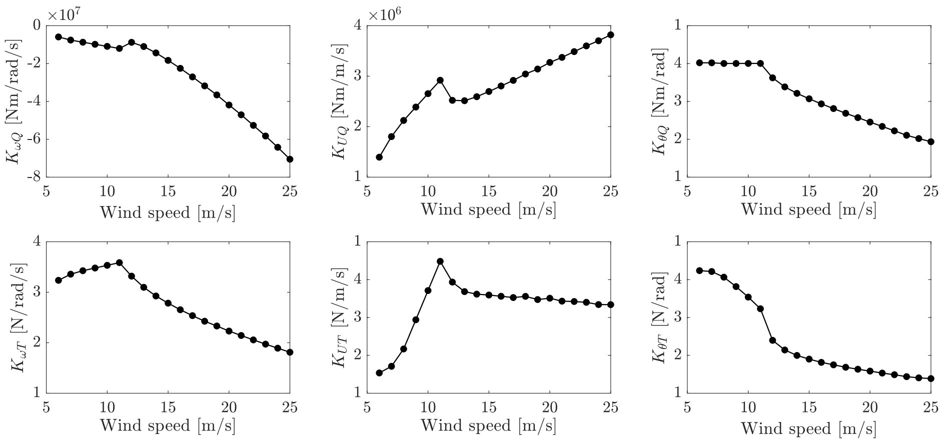

Figure 3. Aerodynamic sensitivities for the DTU 10MW reference wind turbine rotor as function of mean wind speed.

3.1. Time domain
The FOWT is simulated in FAST for 2400 s of zero-degree irregular waves generated according to the JONSWAP spectrum (significant height H_s 1.265 m, peak period T_p 10 s) and a constant and uniform wind with a mean speed of 10 m/s (below-rated) and 18 m/s (above-rated), respectively. The wind turbine generator and collective pitch angle are controlled according to the same variable-speed variable-pitch strategy that achieves speed and power regulation. The linear model is then simulated with the wave elevation, horizontal turbulence, collective pitch request and generator torque request from the corresponding FAST runs as inputs. The output of the two models is compared in terms of rotor speed deviation from the steady-state value and platform DOFs motion with respect to the static equilibrium position (perturbed response). Outputs of the last 200 s of the simulations are illustrated in figure 4-5.

The proposed wave-excited linear model matches the FAST simulations well concerning rotor speed, platform surge and platform pitch motions. Some differences are present in the platform heave and yaw DOFs responses. For the heave motion these could be ascribed to the wave loads that are modeled according to two different approaches by the two models. Especially, it appears that the wave heave force is under-predicted by the WEM included in the linear model. For the yaw motion, differences could be due to the yaw gyroscopic moment effect that is neglected in the linear model. For the considered load cases, the response of the platform sway and roll DOFs is negligible.

3.2. Frequency domain
In addition to the time-domain simulations, the frequency-domain comparisons are presented for discussions. The wave disturbance transfer functions for the platform surge $G_{\eta x}$ and platform pitch $G_{\eta\beta}$ are computed from the linear model for a mean wind speed of 10 m/s and 18 m/s. In figure 6, the transfer functions are compared in terms of magnitude to the response-amplitude-operators (RAOs) for the same platform DOFs and operation condition obtained from FAST. RAOs were computed from time-domain simulation of the FOWT response to white noise waves for 10000 s.

The agreement is good in the 0-0.1 Hz frequency range. The amplitude of the platform pitch response at the surge mode frequency (around 0.01 Hz) for the linear model is greater than for FAST. This could be due to a different damping of the surge mode or a different magnitude of the wave excitation forces in this frequency range.

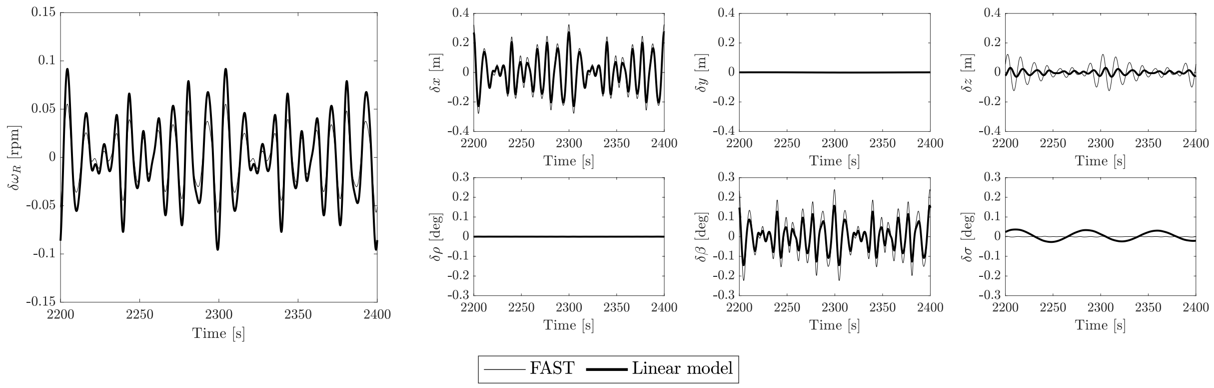

Figure 4. Rotor speed (left) and platform DOFs (right) perturbed response to irregular waves (significant height H_s 1.265 m, peak period T_p 10 s) for a mean wind speed of 10 m/s.

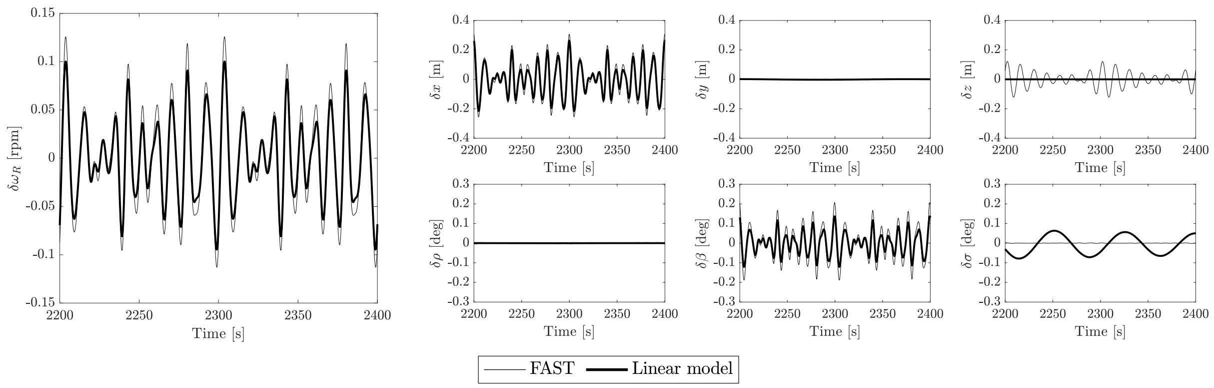

Figure 5. Rotor speed (left) and platform DOFs (right) perturbed response to irregular waves (significant height H_s 1.265 m, peak period T_p 10 s) for a mean wind speed of 18 m/s.

4. FOWT plant linear analysis

The FOWT representation from the linear model can be readily used for control design purposes. This is proved using the model for investigating the implementation of a control strategy for above-rated power regulation based on collective pitch-to-feather. A number of past studies, like [21, 22, 23], evidenced that the pitch controller may interact with the FOWT low-frequency rigid-body modes, resulting in large motions and excessive fatigue loads for the system components. The reasons behind this unstable behavior are difficult to understand from time-domain simulations but are particularly clear from a linear analysis of the FOWT. The transfer function from collective pitch angle to rotor speed $G_{\theta\omega}$, which represents the plant for the pitch controller, is studied for different above-rated wind speeds. A portion of the pole-zero map of $G_{\theta\omega}$ is shown on the left of figure 7. The platform pitch mode is associated with a pair of complex conjugate poles and zeros that move in the complex plane for increasing wind speed. The platform pitch zeros remain in the right-hand-side plane for wind speeds up to 18 m/s, causing the large phase loss in $G_{\theta\omega}$ that is evident in the magnitude-phase plot on the right of figure 7.

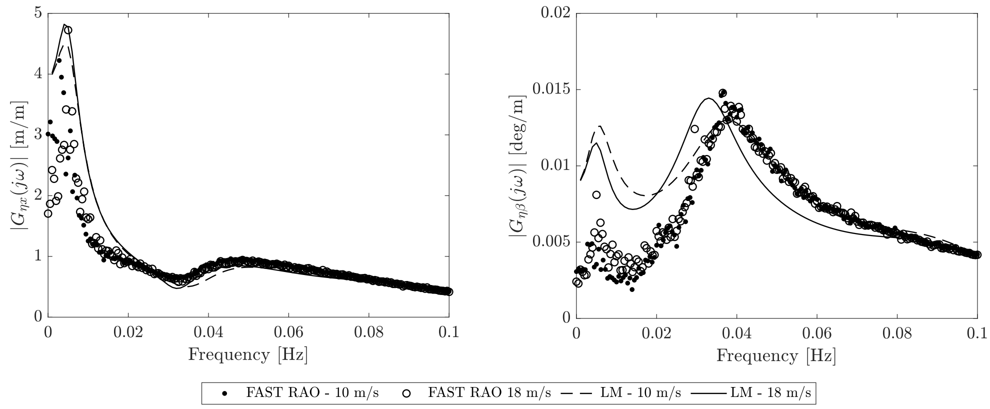

Figure 6. Wave disturbance dynamics for the platform surge (left) and platform pitch (right) for two wind turbine operation conditions (mean wind speed of 10 m/s and 18 m/s). Comparison between FAST response amplitude operators (RAO) and linear model (LM).

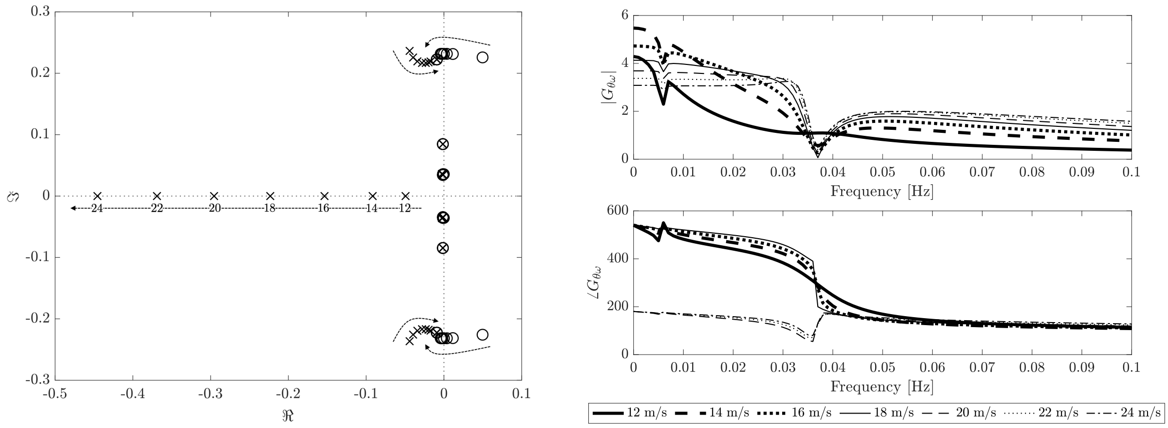

Figure 7. Wind turbine pitch controller plant $G_{\theta\omega}$ (transfer function from collective pitch angle to rotor speed) in above-rated operation conditions. Left: pole-zero map; for increasing wind speed poles ($\times$) and zeros ($\bigcirc$) move in the complex plane as shown by the dashed arrows. Right: magnitude-phase plot.

5. Conclusions

Floating wind is a promising technology for harvesting the abundant wind energy resource in deep waters. Controlling a wind turbine mounted on a floating foundation is challenging and new control strategies have to be developed in order to maximize power production and to reduce fatigue loads. Control-oriented models are needed to solve this task but are currently lacking.

In this paper, a control-oriented wave-excited linear model for FOWTs is developed and verified against the high-fidelity time-domain-based counterpart FAST v8.16. In general, the proposed model shows good performance in describing the FOWT dynamics. In particular, the responses of rotor and platform modes to the disturbances introduced by wind turbulence, waves and to the main wind turbine control inputs (i.e. generator torque and collective pitch angle), match the high-fidelity simulation well. Furthermore, the FOWT representation from the linear model can be readily included into the most common control design algorithms and can be used for the design of observers as well.

6. Acknowledgements

This project has partially received funding from the European Unions Horizon 2020 Programme *Low-cost, low-carbon energy supply* under grant agreement No 815083, and Marie Sklodowska-Curie Action (Project EDOWE, grant 835901).

References

[1] A. Pegalajar-Jurado, M. Borg, and H. Bredmose. An efficient frequency-domain model for quick load analysis of floating offshore wind turbines. *Wind Energy Science Discussions*, pages 1–30, 04 2018.

[2] J.R. Homer and R. Nagamune. Physics-based 3-D control-oriented modeling of floating wind turbines. *IEEE Transactions on Control Systems Technology*, 26(1):14–26, 2018.

[3] F. Lemmer, D. Schlipf, D. Matha, and P.W. Cheng. Integrated optimization of floating wind turbine systems. volume 9, 08 2015.

[4] Z. Lin, D. Cevasco, and M. Collu. A methodology to develop reduced-order models to support the operation and maintenance of offshore wind turbines. *Applied Energy*, 259, 2020.

[5] Ahmed A. Shabana. Flexible multibody dynamics: Review of past and recent developments. *Multibody System Dynamics*, 1(2):189–222, 1997.

[6] M. Hall and A. Goupee. Validation of a lumped-mass mooring line model with DeepCwind semisubmersible model test data. *Ocean Engineering*, 104:590–603, 2015.

[7] F.F. Wendt, M.T. Andersen, A.N. Robertson, and J.M. Jonkman. Verification and validation of the new dynamic mooring modules available in FAST v8. volume 2016-January, pages 352–363, 2016.

[8] Jason Jonkman. Dynamics modeling and loads analysis of an offshore floating wind turbine. 01 2007.

[9] José Azcona Armendáriz. *Computational and Experimental Modelling of Mooring Lines Dynamics for Offshore Floating Wind Turbines.* PhD thesis, December 2015.

[10] W. Cummins. The impulse response function and ship motion. technical report 1661, david taylor model basindtnsrdc. 1962.

[11] T.F. Ogilvie. Recent progress toward the understanding and prediction of ship motions. In *5th Symposium on Naval Hydrodynamics, Bergen, Norway*, pages 3–80, 1964.

[12] R. Beck and A. Reed. Modern computational methods for ships in seaway. *Transactions of Society of Naval and Marine Engineers*, 109, 01 2001.

[13] T. Perez and T. Fossen. A Matlab toolbox for parametric identification of radiation-force models of ships and offshore structures. *Modeling, Identification and Control*, 30, 01 2009.

[14] F. Lemmer, S. Raach, D. Schlipf, and P.W. Cheng. Parametric wave excitation model for floating wind turbines. volume 94, pages 290–305, 2016.

[15] J. Falnes. On non-causal impulse response functions related to propagating water waves. *Applied Ocean Research*, 17(6):379–389, 1995.

[16] A. Fontanella, I. Bayati, and M. Belloli. Linear coupled model for floating wind turbine control. *Wind Engineering*, 42(2):115–127, 2018.

[17] Frank Lemmer. Low-order modeling, controller design and optimization of floating offshore wind turbines. page 224, 2018.

[18] F.D. Bianchi, H. de Battista, and R.J. Mantz. *Wind Turbine Control Systems.* Springer, 2007.

[19] C. Bak, F. Zahle, R. Bitsche, T. Kim, A. Yde, L.C. Henriksen, M.H. Hansen, J.P.A.A. Blasques, G. Mac, and N. Anand. The DTU 10-MW reference wind turbine, 2013.

[20] J. Azcona, F. Vittori, U.S. Paulsen, F. Savenije, G. Kapogiannis, X. Karvelas, D. Manolas, S. Voutsinas, F. Amann, R. Faerron Guzman, and F. Lemmer. Design solutions for 10MW floating offshore wind turbines. deliverable 4.37. INNWIND.eu., 2017.

[21] J. Jonkman, S. Butterfield, W. Musial, and G. Scott. Definition of 5-MW Reference Wind Turbine for Offshore System Development. *Technical Report NREL/TP-500-38060*, 2009.

[22] T.J. Larsen and T.D. Hanson. A method to avoid negative damped low frequent tower vibrations for a floating, pitch controlled wind turbine. volume 75, 2007.

[23] G.J. van der Veen, I.J. Couchman, and R.O. Bowyer. Control of floating wind turbines. In *2012 American Control Conference (ACC)*, pages 3148–3153, 06 2012.